Journal of Dentistry 150 (2024) 105310

Contents lists available at ScienceDirect

Journal of Dentistry

journal homepage: www.elsevier.com/locate/jdent

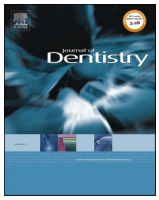

Influence of scanning pattern on accuracy, time, and number of photograms of complete-arch implant scans: A clinical study

Miguel Gómez-Polo [a,*], Rocío Cascos [b], Rocío Ortega [c], Abdul B. Barmak [d], John C. Kois [e], Jorge Alonso Pérez-Barquero [f], Marta Revilla-León [g]

[a] Associate Professor Department of Conservative Dentistry and Prosthodontics, Complutense University of Madrid, Madrid, Spain, Director of Postgraduate Program of Advanced in Implant-Prosthodontics, School of Dentistry, Complutense University of Madrid, Madrid, Spain
[b] Student Postgraduate Program of Advanced in Implant-Prosthodontics, School of Dentistry, Complutense University of Madrid, Madrid, Spain
[c] Adjunct Professor Department of Prosthetic Dentistry, School of Dentistry, European University of Madrid, Madrid, Spain
[d] Assistant Professor Clinical Research and Biostatistics, Eastman Institute of Oral Health, University of Rochester Medical Center, Rochester, NY, USA
[e] Kois Center, Private Practice, Seattle, Wash and Assistant Professor, Graduate Prosthodontics, School of Dentistry, University of Washington, Seattle, Wash, USA
[f] Adjunct Professor, Department of Dental Medicine, Faculty of Medicine and Dentistry, University of Valencia, Valencia, Spain
[g] Affiliate Assistant Professor, Graduate Prosthodontics, Department of Restorative Dentistry, School of Dentistry, University of Washington, Seattle, WA; Faculty and Director of Research and Digital Dentistry, Kois Center, Seattle, WA; and Adjunct Professor, Department of Prosthodontics, School of Dental Medicine, Tufts University, Boston, MA, USA

ARTICLE INFO

Keywords:
Accuracy
Digital impression
Intraoral scanner
Implant scan
Scanning pattern

ABSTRACT

Objectives: To measure the influence of scanning pattern on the accuracy, time, and number of photograms of complete-arch intraoral implant scans.
Methods: A maxillary edentulous patient with 7 implants was selected. The reference implant cast was obtained using conventional methods (7Series Scanner). Four groups were created based on the scanning pattern used to acquire the complete-arch implant scans by using an intraoral scanner (IOS) (Trios4): manufacturer's recommended (Occlusal-Buccal-Lingual (OBL)), zig-zag (Zig-zag), circumferential (Circumf), and novel pattern that included locking an initial occlusal scan (O-Lock group) ($n = 15$). Scanning time and number of photograms were recorded. The linear and angular measurements were used to assess scanning accuracy. One-way ANOVA and Tukey tests were used to analyze trueness, scanning time, and number of photograms. The Levene test was selected to assess precision (α=0.05).
Results: Statistically significant differences in trueness were detected among OBL, Zig-zag, Circumf, and O-Lock regarding linear discrepancy ($P < 0.01$), angular discrepancy ($P < 0.01$), scanning time ($P < 0.01$), and number of photograms ($P < 0.01$). The O-Lock (63 ± 20 μm) showed the best linear trueness with statistically significant differences ($P < 0.01$) with Circumferential (86 ± 16 μm) and OBL (87 ± 19 μm) groups. The O-Lock (93.5 ± 13.4 s, 1080 ± 104 photograms) and Circumf groups (102.9 ± 15.1 s, 1112 ± 179 photograms) obtained lower scanning times ($P < 0.01$) and number of photograms ($P < 0.01$) than OBL (130.3 ± 19.4 s, 1293 ± 161 photograms) and Zig-zag (125.7 ± 22.1 s, 1316 ± 160 photograms) groups.
Conclusions: The scanning patterns tested influenced scanning accuracy, time, and number of photograms of the complete-arch scans obtained by using the IOS tested. The zig-zag and O-Lock scanning patterns are recommended to obtain complete-arch implant scans when using the selected IOS.

1. Introduction

The accuracy of definitive implant casts is fundamental for fabricating complete-arch implant-supported prostheses [1,2]. Dental literature has identified different factors that can impact the accuracy of definitive implant casts obtained by using conventional impression methods, namely impression technique [3], implant angulation [4,5], impression material type [6] and its polymerization shrinkage [7-9], and pouring of the dental impression [7-9].

Digital data acquisition technologies such as intraoral scanners

* Corresponding author at: Pza. Ramón y Cajal s/n. School of Dentistry, Complutense University of Madrid. Zip Code: 28033, Madrid, Spain.
E-mail address: mgomezpo@ucm.es (M. Gómez-Polo).

https://doi.org/10.1016/j.jdent.2024.105310
Received 9 February 2024; Received in revised form 1 August 2024; Accepted 12 August 2024
Available online 15 August 2024

(IOSs) and photogrammetry systems [10,11] have enabled the obtention of virtual definitive implant casts [12-17]. Similarly, as in conventional methods, it is important to understand the operator- and patient-related factors [18,19] that can reduce the scanning accuracy of intraoral implant scans [20]. Among these factors, scanning pattern or the sequence at which the intraoral scan is acquired is an operator-related factor that can reduce the accuracy of the intraoral implant scans [20].

Limited dental literature has analyzed the impact of different scanning patterns on the accuracy of complete-arch intraoral implant scans [21,22]. These laboratory investigations demonstrated that if the scanning pattern is changed, the accuracy of the complete-arch intraoral implant scans would vary [21-25]. However, the optimal scanning pattern for complete-arch intraoral implant digital scans remains unclear, due to heterogeneity among the studies. Additionally, only in vitro investigations are available. Therefore, it is unclear if the scanning pattern would impact in the same manner when complete-arch intraoral implant scans are acquired in the patient's mouth.

Previous studies have analyzed the impact of rescanning and locking an existing scan when performing rescanning techniques on the scanning accuracy of IOSs [26-29]. The results of these studies demonstrated that rescanning procedures reduce scanning accuracy of IOSs [26-29]. Additionally, locking the existing scan prior to rescanning improves the accuracy of the intraoral scan [26-29]. However, the impact of this locking procedure on the accuracy of complete-arch implant scans is unknown.

The purpose of this in vitro study was to evaluate the influence of four different scanning patterns (manufacturer's recommended (Occlusal-Buccal-Lingual (OBL)), zig-zag, circumferential, and a novel scanning pattern) on the accuracy (trueness and precision), scanning time, and number of photograms of complete-arch implant scans acquired by using an IOS (Trios 4; 3Shape A/S, Copenhagen, Denmark). The present study analyzed the accuracy of a novel scanning pattern that included locking an initial occlusal scan for acquiring the complete-arch implant scan. This scanning strategy aims to improve implant digital scans accuracy by avoiding the stitching procedure across the complete arch. It will be further described in the Material and Methods section. The null hypotheses were: 1, that there would be no trueness discrepancies between the complete-arch intraoral implant digital scans acquired with different scanning patterns; 2, that there would be no precision discrepancies between the complete-arch intraoral implant digital scans acquired with different scanning patterns; 3, that there would be no difference in the scanning time between the complete-arch intraoral implant digital scans acquired with different scanning patterns; and 4, that there would be no difference in the number of photograms between the complete-arch intraoral implant digital scans acquired with different scanning patterns.

2. Materials and methods

The protocol of the present investigation was reviewed and approved by an ethical committee (22/645-E). The clinical study involved the collection of complete-arch intraoral implant scans with different scanning strategies. The inclusive criteria included an individual older than 18-years in good medical conditions or with mild systemic disease (ASA Type I or II). Additionally, the individual should have between 4 and 8 implants in the edentulous maxillary or mandibular arch in healthy conditions. Patients with limited opening or with peri-implantitis were considered as not eligible for the present investigation. Screening procedures were completed by an experienced restorative dentist. The selected individual volunteered to participate on the present study and a signed informed consent was obtained.

A patient with 7 dental implants placed in the maxillary arch was selected. The dental implants were located in the left second molar, right and left first premolar, left canine, right and left lateral incisor, and right first molar positions. Each implant had an implant abutment (Transepithelial Abutment IC 3.5/4.1 GH3; Avinent Implant System, Barcelona, Spain). The patient had a maxillary screw-retained interim implant-supported prosthesis.

A conventional maxillary complete-arch implant impression was obtained. First, the implant-supported interim prosthesis was removed, and a brand new implant impression abutment was hand-torqued on each implant abutment (Impression Coping Open Tray Transepithelial 4.8 Non-Eng; Avinent Implant System, Barcelona, Spain) (Fig. 1A). The preliminary conventional impression was poured following conventional methods. Then, an implant abutment analog (Transepithelial implant analog model; Avinent Implant System) was positioned on each implant impression abutment. Tissue moulage (Gi-Mask; Coltene, Altstätten, Switzerland) and Type IV dental stone (GC Fujirock EP; GC, Lucerne, Switzerland) with a setting expansion of 0,09 % were used to pour the impression. The dental stone was mixed with water (22 mL of water per each 100 g of dental stone) under vacuum for 30 s, as per manufacturer recommendations. A splinting framework was milled in a polymethyl methacrylate material (CAD/CAD Idodentine disk; Unidesa, Madrid, Spain) by using an additive manufacturing technology (Microlay Versus 385; Microlay, Madrid, Spain) (Fig. 1B) [30,31]. Additionally, a custom tray was manufactured using light photopolymerizing material (Kiero Planchas Tray; Kuss dental, Madrid, Spain).

A brand new implant impression abutment was then hand torqued on each implant abutment (Impression Coping Open Tray Transepithelial 4.8 Non-Eng; Avinent Implant System) following the manufacturer's recommendations, for acquiring the definitive implant impression. The printed framework was connected to the implant impression abutments by using photopolymerizing resin (Conlight; Kuss dental) (Fig. 1C). After the complete polymerization of the resin, the custom open tray was used to obtain the polyether impression (Impregum; 3 M ESPE, Bayern, Germany) with an elastic recovery of 98,7 %. Lastly, after the polymerization of the polyether material, the impression was removed from the patient's mouth. The definitive impression was poured following the same methodology as the preliminary impression. The definitive implant stone cast was kept at 23 °C for 48 h (Fig. 1D).

The definitive implant stone cast was digitized by using a laboratory scanner (E4 Desktop Scanner; 3Shape A/S) (accuracy: 4 μm) [32]. The scanner was previously calibrated as per manufacturer's instructions. A brand-new implant scan body (ISB) (transepithelial scan body 2800; Avinent Implant System) was positioned and tightened to 10 Ncm by using a torque wrench following the manufacturer's recommendations on each implant abutment of the definitive implant cast. The implant scan body geometry bevel feature was oriented towards the lingual surface [33]. Then, the laboratory scan was acquired. The standard tessellation language (STL) file was exported.

A dental computer-aided design (CAD) software program (DentalCAD 3.1, Rijeka; Exocad GmbH, Darmstadt Germany) was used to design an implant-supported bar. First, the STL file of the digitized definitive implant stone cast was imported. The virtual definitive implant cast was obtained by aligning the CAD object of the ISB with each ISB of the STL file. Subsequently, the CAD tools were used to design an implant-supported bar (Fig. 2A). The bar designed was used to fabricate a milled (PrograMill PM7; Ivoclar Vivadent, Zurich, Switzerland) titanium grade 5 (Colado CAD Ti5 Disc; Ivoclar Vivadent) implant-supported bar (Fig. 2B). The fit of the implant-supported bar was checked in the definitive implant stone cast and patient's mouth by using the Sheffield's test (Fig. 3). Periapical radiographs were obtained.

Four groups were created based on the scanning pattern used to acquire the complete-arch intraoral implant scan by using an IOS (Trios 4, v.22.2 3Shape A/S): scanning pattern recommended by the IOS manufacturer for scanning completely dentate patients (OBL group), zig-zag scanning pattern (Zig-zag group), circumferential scanning pattern (Circumf group), and a novel scanning pattern that included locking the initial occlusal scan (O-Lock group) ($n = 15$). The IOS selected was previously calibrated by using the manufacturer's recommended protocol [34]. A brand-new ISB (transepithelial scan body 2800; Avinent Implant System) was placed on each implant abutment of

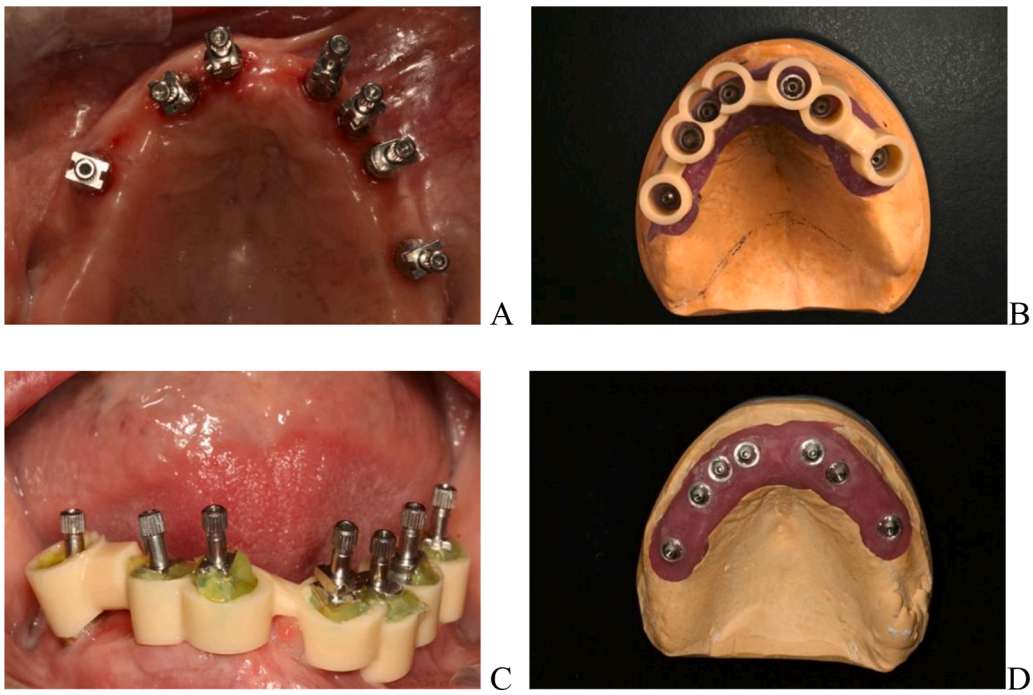

Fig. 1. Conventional maxillary complete-arch implant impression procedures. A, Implant impression abutments placed. B, Splinting framework. C, Implant impression abutments joined to the splinting framework. D, Definitive implant cast.

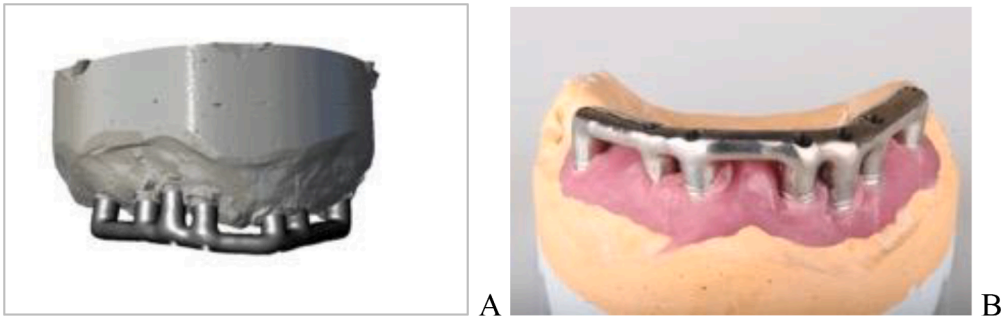

Fig. 2. A, Design of implant-supported bar on the virtual definitive implant cast. B, Milled implant-supported bar.

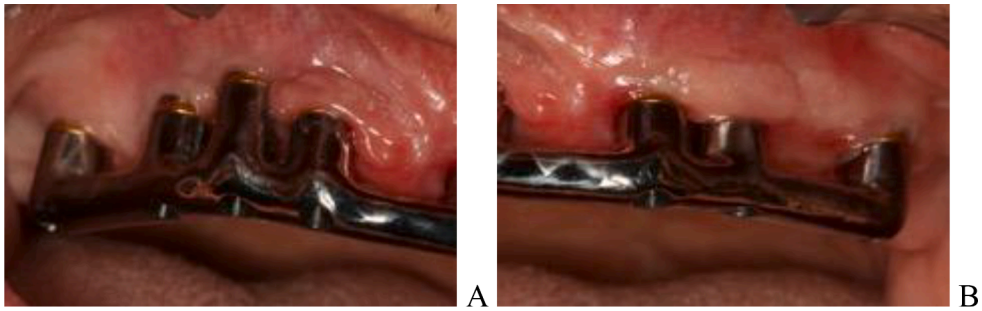

Fig. 3. Clinical evaluation of the milled titanium implant-supported bar. A, Maxillary right quadrant. B, Maxillary left quadrant.

the patient by following the manufacturer's recommendations [35]. The ISBs were not splinted. Additionally, the ISBs were maintained in the same position until all the data acquisition procedures of the same group were completed. Sample size was determined based on previous studies with similar methodology [21,36-38].

All the intraoral digital implant scans were recorded by a restorative dentist with more than 10 years of previous experience handling IOSs (M.G-P) [38,39]. Intraoral implant scans were captured in a room without windows and a dental chair [40,41]. Ambient lighting illumination at the patient's mouth was 1000-lux [42,43] measured by using a luxmeter (LX1330B Light Meter; Dr. Meter Digital Illuminance, Union City, USA). The complete-arch intraoral implant scans always started on the implant positioned in the right second molar of the patient for all subgroups. Additionally, the palate was not included in the scans, as its inclusion does not significantly impact the accuracy of complete-arch intraoral images [44]. Rescanning procedures were avoided [24,28,

29]. The scanning time and number of photograms for each specimen were registered, as provided by the software program of the IOS selected.

In the Circumf group, the scan stared on the occlusal surface of the ISB positioned on the right first molar, which was then completely scanned by moving the IOS in a circular motion around the circumference of the ISB. Next, in an anterior movement towards the contralateral ISB, the remaining ISB were digitized in a similar circular circumferential motion [45] (Fig. 4A).

In the O-Lock group, the intraoral scan started on the occlusal surface of the ISB positioned on the right first molar. Then, the occluso-lingual surfaces of the ISBs were scanned towards the contralateral ISB. The objective is to record as much ISBs surface as possible including the smaller number of photograms. This is the reason to perform the first movement by the inner part of the arch, trying to the reduce the accumulation of inaccuracies due to the stitching. [46,47] Subsequently, the scanning process was stopped, and the ISB surfaces registered were locked by using the "lock" tool of the IOS software program [29]. It aims to avoid the modification of the ISBśpositions during the remaining scanning procedure, The second step started in the registered surface of the ISB positioned in the right first molar. From this point, the IOS was moved by the interproximal and vestibular surfaces until the complete record of the ISB (Fig. 4B). Then, the scanner advanced, recording the soft tissues and the entire surfaces of all the ISBs.

In the OBL group, the scanning pattern started on the occlusal surface of the ISB positioned on the right first molar and moved towards the occlusal surface of the ISB positioned on the left second molar. Then, the IOS was rotated towards the buccal surface, and the buccal surfaces from the ISB positioned on the left second molar towards the right first molar were digitized. Afterwards, the IOS was rotated towards the lingual surface, and the lingual surfaces from the ISB located on the left second molar to the right first molar were scanned (Fig. 4C). This procedure was repeated until specimens were captured.

In the Zig-zag group, the scan started on the occlusal surface of the ISB positioned on the right first molar, then moving the IOS in a zig-zag motion towards the contralateral ISB, the occlusal, buccal, and lingual surfaces were digitized [48-50] (Fig. 4D).

The digitized definitive implant cast (reference STL file) was used as a reference to measure the discrepancy with the experimental scans obtained among the different groups tested. The reference STL file was imported into a reverse engineering software program (Geomagic Control X; 3D Systems, Rock Hill, USA). A CAD cylinder geometry was aligned with each ISB of the reference file using the best fit technique [51]. The longitudinal axis of each ISB was located, followed by marking the z-plane positioned on the most apical surface of each ISB. The intersection between the longitudinal axis and z-plane of each ISB was determined as the measurement point. Linear and angular measurements among the seven ISBs were calculated (Fig 5A and B). The same procedures were completed on each experimental scan. The linear and angular measurements obtained on the reference file was used to calculate the discrepancies with each experimental scan. The 6 ISB linear and angular discrepancies were averaged per scan before averaging the 15 scans for each group. Trueness was defined as the linear and angular discrepancies between the reference and experimental scans [52,53]. Precision was described as the linear and angular variations per each group. It was determined by the standard deviation (SD) [52,53].

The Kolmogorov-Smirnov test was employed to evaluate the normality of the sample for each variable. These tests revealed that the linear and angular discrepancies, scanning time, and number of photograms data were normally distributed ($P > 0.05$). (Table 1) One-way ANOVA, followed by the pairwise comparison Tukey tests were used to analyze the linear and angular trueness, scanning time, and number of photograms data. The Levene test was used to analyze the linear and angular precision. The statistical analysis was performed by using a statistical software program (IBM SPSS Statistics for Windows, v26; IBM Corp) ($\alpha = 0.05$).

3. Results

The trueness and precision values, scanning time, and number of photograms obtained among the groups tested are presented in Table 2. Regarding linear trueness, one-way ANOVA showed significant linear trueness differences among the groups tested (df = 3, MS=0.00183673, $F = 6.79$, $P < 0.01$) (Table 3). Tukey test revealed significant linear trueness discrepancies among the groups tested, being the Circumf and O-Lock groups ($P < 0.01$) and OBL and Zig-zag groups ($P < 0.01$) significantly different from each other (Fig. 6A) (Table 4). Hence, the zig-zag and O-Lock groups had the best linear trueness among the groups

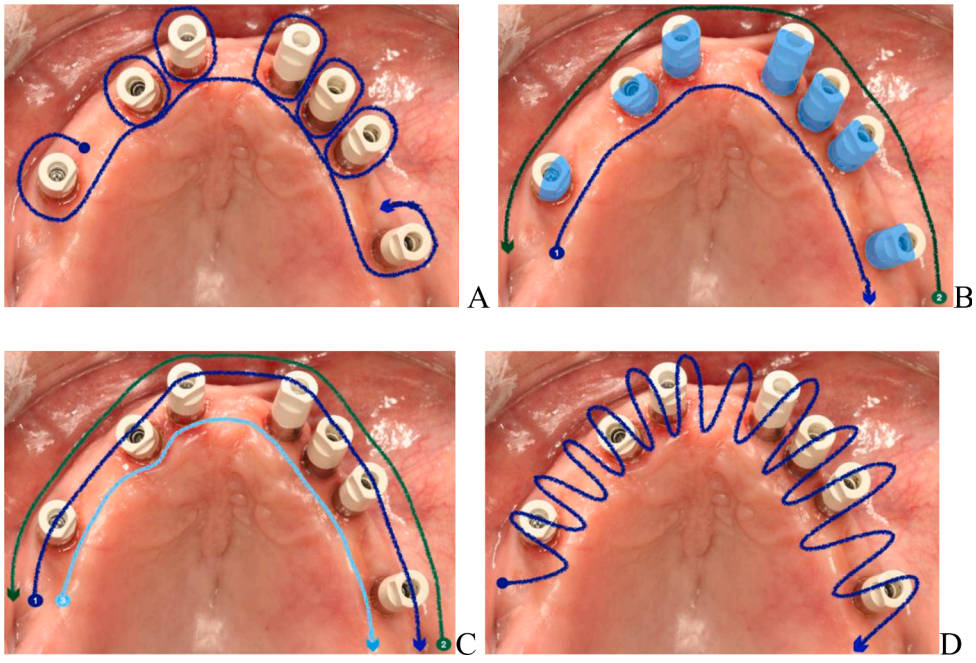

Fig. 4. Scanning patterns tested. A, Circumferential. B, O-Lock. C, OBL. D, Zig-zag.

Fig. 5. Representative figures of linear and angular measurements among ISBs. A, Linear measurements. B, Angular measurements.

Table 1
Normality tests conducted for the studied variables.

Normality Tests		statistic	p
Linear Distance	Kolmogorov-Smirnov	0.102	0.559
Angular Distance	Kolmogorov-Smirnov	0.133	0.238
Scanning Time	Kolmogorov-Smirnov	0.0746	0.892
No. of Photograms	Kolmogorov-Smirnov	0.0855	0.773

Table 2
Trueness and precision values, scanning time, and number of photograms measured among the subgroups tested.

Group	Mean ±SD linear discrepancies (μm)	Mean ±SD angular discrepancies (degrees)	Mean ±SD scanning time (seconds)	Mean ±SD number of photograms
Circumf	86 ± 16^{B}	0.60 ± 0.15^{B}	102.9 ± 15.1 ^{A}	1112 ± 179 ^{A}
O-Lock	63 ± 20^{A}	0.62 ± 0.08^{B}	93.5 ± 13.4 ^{A}	1080 ± 104 ^{A}
OBL	87 ± 19 ^{B}	0.84 ± 0.29 ^{C}	130.3 ± 19.4 ^{B}	1293 ± 161 ^{B}
Zig-zag	78 ± 8 ^{AB}	0.43 ± 0.05^{A}	125.7 ± 22.1 ^{B}	1316 ± 160 ^{B}

B, buccal; Circumf, circumferential; L, lingual; O, occlusal; SD, standard deviation. Groups with same superscript letter (within column) indicate not significantly different ($P > 0.05$).

Table 3
ANOVA table for linear distance discrepancies.

Source	DF	Sum of Squares	Mean Square	F Value	Pr > *F*
Model	3	0.00551018	0.00183673	6.79	0.0006
Error	56	0.01514680	0.00027048		
Corrected Total	59	0.02065698			

B, buccal; Circumf, circumferential; L, lingual; O, occlusal; DF, degrees of freedom.

tested. However, Levene test revealed no difference on the linear precision values among the groups tested ($P = 0.34$) (Table 5).

Regarding angular trueness, one-way ANOVA showed significant angular trueness differences among the groups tested (df = 3, MS = 0.42383855, $F = 14.59$, $P < 0.01$) (Table 6). Tukey test revealed significant angular trueness discrepancies among the groups tested, being the Circumf and OBL groups ($P < 0.01$), Circumf and Zig-zag groups ($P < 0.05$), O-Lock and OBL groups ($P < 0.01$), O-Lock and Zig-zag groups ($P < 0.01$), OBL and Zig-zag groups ($P < 0.001$) significantly different from each other (Fig. 6B) (Table 7). Thus, the zig-zag group obtained the best angular trueness among the groups tested. However, Levene test revealed no difference on the precision values among the groups tested ($P = 0.25$). (Table 8)

Regarding scanning time, one-way ANOVA demonstrated significant scanning time differences among the groups tested (df=3, MS=4694.15556, $F = 14.74$, $P < 0.01$) (Table 9). The Tukey test showed significant scanning time differences among the groups tested, being the Circumf and OBL groups ($P < 0.01$), Circumf and Zig-zag groups ($P < 0.01$), O-Lock and OBL groups ($P < 0.01$), O-Lock and Zig-zag groups ($P < 0.01$) significantly different from each other (Fig. 6C) (Table 10). Therefore, the O-Lock group obtained the lowest scanning time among the groups tested.

Regarding the number of photograms, one-way ANOVA revealed significant differences in the number of photograms across the subgroups tested (df = 1, MS = 221,512.222, $F = 9.40$, $P < 0.01$) (Table 11) Tukey test showed significant differences in the number of photograms between the groups tested, being the Circumf and OBL groups ($P < 0.05$), Circumf and Zig-zag groups ($P < 0.01$), O-Lock and OBL groups ($P < 0.01$), O-Lock and Zig-zag groups ($P < 0.01$) significantly different from each other (Fig. 6D) (Table 12). Therefore, the O-Lock group obtained the smallest number of photograms among the groups tested.

4. Discussion

Based on the results obtained, the scanning patterns tested significantly impacted the scanning trueness, scanning time, and number of photograms of the complete-arch implant scans acquired by using the IOS selected. Therefore, the second null hypothesis was accepted, while the remaining three null hypotheses were rejected.

Based on the results of the present clinical study, the linear trueness ±precision ranged from 63 ± 20 to 87 ± 16 μm, while the angular trueness ±precision ranged from 0.43 ± 0.05 to 0.84 ± 0.29 degrees. Dental literature has reported that the clinically acceptable discrepancy of the implant-prosthodontic gap is 150 μm [54,55]. Nevertheless, the results obtained in this study should be interpretated with caution, as the linear distance between platforms was determined instead for the linear deviation in the platform [46]. The fit of the implant framework is the result of the distortion obtained during the fabrication of the conventional or virtual definitive implant cast and the manufacturing techniques of the implant-supported prostheses. The clinically acceptable discrepancy threshold for complete-arch implant impressions or definitive implants casts is uncertain [54,55]. However, the scanning distortion should be below the acceptable discrepancy of the implant-prosthodontic gap [56]. In the present study, the scanning distortion measured in all groups was significantly lower than the clinically acceptable discrepancy of the implant-prosthodontic gap.

In the present study, the zig-zag and O-Lock scanning patterns tested demonstrated the best linear trueness values when compared with the OBL and circumferential scanning patterns. However, the zig-zag scanning pattern obtained significantly better angular trueness when compared with the O-Lock scanning pattern; nonetheless, only a 0.12 degrees mean discrepancy was observed between both scanning patterns. Additionally, although the zig-zag technique reported lower values (8 μm) than the other techniques (16–20 μm), the scanning patterns tested did not significantly impact the precision values of the IOS

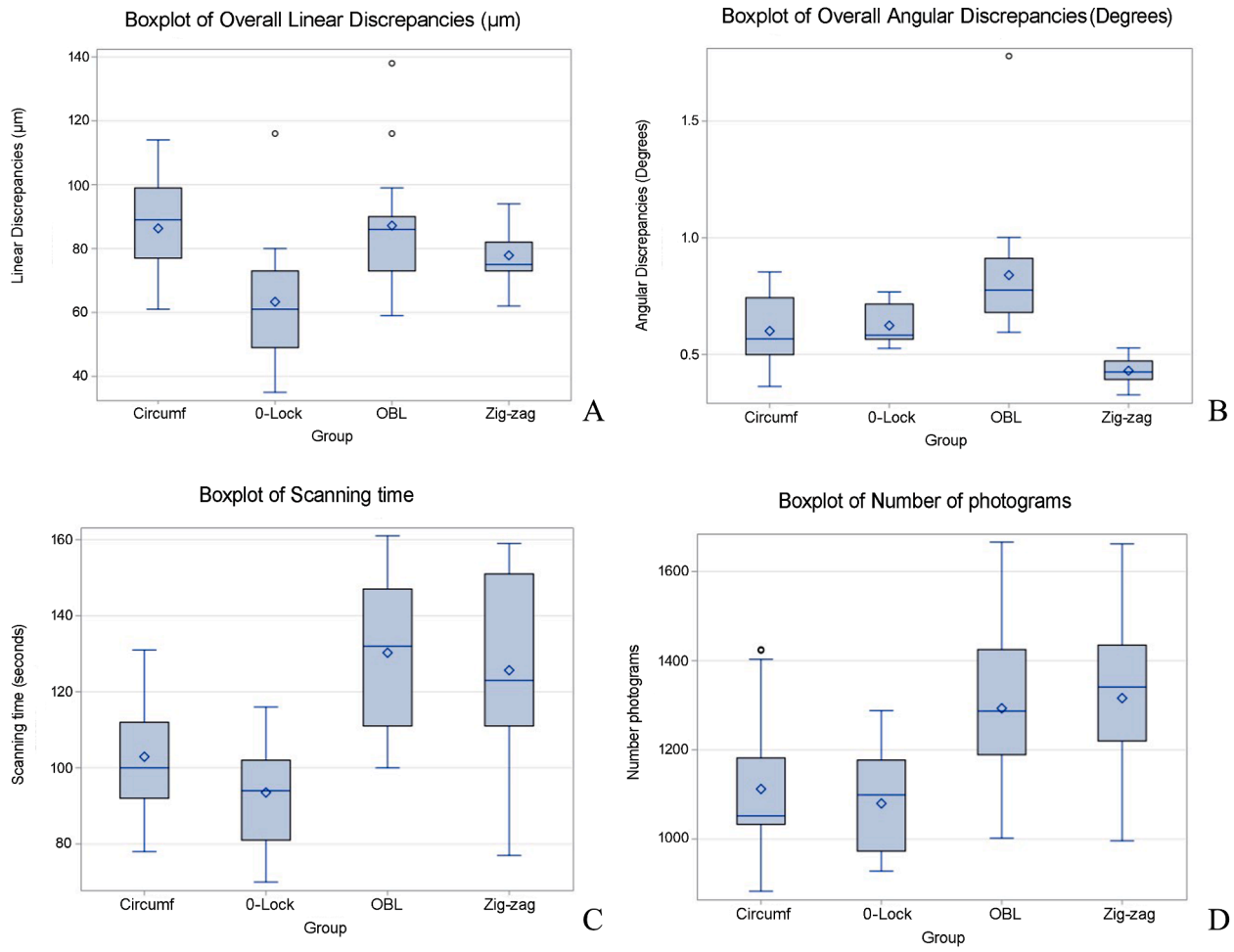

Fig. 6. A, Boxplot of linear discrepancies measured among the groups tested. B, Boxplot of angular discrepancies measured among the groups tested. C, Boxplot of scanning time measured among the groups tested. D, Boxplot of number of photograms measured among the groups tested.

Table 4
Tukey test for linear distance discrepancies. Significant differences highlighted in bold.

Least Squares Means for effect Group LSMean(i)=LSMean(j)				
i/j	Circumf	O-Lock	OBL	Zig-zag
Circumf		**0.0018**	0.9989	0.4986
O-Lock	**0.0018**		**0.0011**	0.0849
OBL	0.9989	**0.0011**		0.4128
Zig-zag	0.4986	0.0849	0.4128	

B, buccal; Circumf, circumferential; L, lingual; O, occlusal; LS, Least Squares.

Table 5
Levene test for linear distance discrepancies.

Levene's Test for Homogeneity of Angular Distance Variance ANOVA of Squared Deviations from Group Means					
Source	DF	Sum of Squares	Mean Square	F Value	Pr > *F*
Group	3	0.0532	0.0177	1.41	0.2494
Error	56	0.7046	0.0126		

B, buccal; Circumf, circumferential; L, lingual; O, occlusal; DF, degrees of freedom.

tested. Therefore, the zig-zag and O-Lock scanning patterns may be recommended to obtain complete-arch implant scans when using the selected IOS (Trios 4; 3Shape A/S), aiming to maximize the accuracy of the virtual definitive implant cast.

Table 6
ANOVA table for angular discrepancies.

Source	DF	Sum of Squares	Mean Square	F Value	Pr > *F*
Model	3	1.27151565	0.42383855	14.59	<0.0001
Error	56	1.62723320	0.02905774		
Corrected Total	59	2.89874885			

DF, degrees of freedom.

Table 7
Tukey test for angular discrepancies. Significant differences highlighted in bold.

Least Squares Means for effect Group LSMean(i)=LSMean(j)				
i/j	Circumf	O-Lock	OBL	Zig-zag
Circumf		0.9819	**0.0017**	**0.0404**
O-Lock	0.9819		**0.0054**	**0.0151**
OBL	**0.0017**	**0.0054**		**<0.0001**
Zig-zag	**0.0404**	**0.0151**	**<0.0001**	

B, buccal; Circumf, circumferential; L, lingual; O, occlusal; LS, Least Squares.

A previous in vitro and clinical studies have shown that rescanning techniques reduce the accuracy of IOSs, but locking the existing scan before rescanning maximizes the accuracy of the procedure [26-29]. In the present investigation, the novel scanning pattern that includes locking an initial occlusal scan for capturing complete-arch implant scans has been tested. This novel scanning pattern obtained similar linear and angular trueness and precision values than the zig-zag

Table 8
Levene test for angular discrepancies.

Levene's Test for Homogeneity of Angular Discrepancies Variance ANOVA of Squared Deviations from Group Means					
Source	DF	Sum of Squares	Mean Square	F Value	Pr > *F*
Group	3	0.0532	0.0177	1.41	0.2494
Error	56	0.7046	0.0126		

DF, degrees of freedom.

Table 9
ANOVA table for scanning time.

Source	DF	Sum of Squares	Mean Square	F Value	Pr > *F*
Model	3	14,082.46667	4694.15556	14.74	<0.0001
Error	56	17,836.93333	318.51667		
Corrected Total	59	31,919.40000			

DF, degrees of freedom.

Table 10
Tukey test for scanning time.

Least Squares Means for effect Group: LSMean(i)=LSMean(j)				
i/j	Circumf	O-Lock	OBL	Zig-zag
Circumf		0.4788	**0.0006**	**0.0051**
O-Lock	0.4788		**<0.0001**	**<0.0001**
OBL	**0.0006**	**<0.0001**		0.8944
Zig-zag	**0.0051**	**<0.0001**	0.8944	

B, buccal; Circumf, circumferential; L, lingual; O, occlusal; LS, Least Squares.

Table 11
ANOVA table for number of photograms.

Source	DF	Sum of Squares	Mean Square	F Value	Pr > *F*
Model	3	664,536.667	221,512.222	9.40	<0.0001
Error	56	1,319,462.667	23,561.833		
Corrected Total	59	1,983,999.333			

DF, degrees of freedom.

Table 12
Tukey test for number of photograms. Significant differences highlighted in bold.

Least Squares Means for effect Group: LSMean(i)=LSMean(j)				
i/j	Circumf	O-Lock	OBL	Zig-zag
Circumf		0.9379	**0.0109**	**0.0033**
O-Lock	0.9379		**0.0019**	**0.0005**
OBL	**0.0109**	**0.0019**		0.9768
Zig-zag	**0.0033**	**0.0005**	0.9768	

B, buccal; Circumf, circumferential; L, lingual; O, occlusal; LS, Least Squares.

scanning pattern. Additionally, the novel scanning pattern assessed obtained the lowest scanning time and number of photograms, which may represent an advantage when compared with the zig-zag scanning pattern.

Two previous in vitro studies have analyzed the influence of the scanning pattern on the accuracy of complete-arch implant scans [21,22]. Due to the heterogeneity on the research methodology among these in vitro studies (reference cast, digitizing method to obtain the control file, IOS system and generation, and measurement method), direct comparisons with the results obtained in the present study is difficult. Additionally, in the best authors' knowledge, this is the first clinical investigation that assessed the impact of four scanning patterns on the accuracy of complete-arch intraoral implant scans.

A previous in vitro study evaluated the influence of different scanning patterns on the accuracy and scanning time of complete-arch maxillary implant scans obtained by using 2 IOSs: Trios 3 from 3Shape A/S and CS 3600 from Carestream [22]. The reference cast had 6 parallel implant abutment analogs that were digitized by using a laboratory scanner (D2000; 3Shape A/S) for capturing the reference or control scan. This study did not include the O-Lock scanning pattern. The results revealed scanning accuracy and scanning time differences among the implant scans acquired with different scanning patterns. Three of the six scanning patterns tested corresponded to the OBL, circumferential, and zig-zag scanning patterns tested in the present study; however, research methodology discrepancies with the present study make difficult the result comparisons between both studies.

Gómez-Polo et al. evaluated the influence of six scanning patterns on the accuracy of maxillary and mandibular complete-arch implant scans obtained by using an IOS (Trios 4, v.21.3; 3Shape A/S) [21]. The six scanning patterns tested included the OBL, circumferential, and zig-zag patterns when scanning a maxillary and mandibular model, having each cast 6 dental implants placed. This study did not consider the O-Lock scanning pattern. Authors reported that the circumferential and OBL scanning patterns obtained the highest accuracy values, while the zig-zag pattern obtained the worse accuracy values among all the groups tested. In the present investigation, the zig-zag scanning pattern obtained higher linear and angular trueness than the OBL and circumferential scanning patterns. This may be explained by the clinical conditions of the present study, IOS software version, different implant position (location in the dental arch, depth, angulation, and inter-implant distance) [57,58], amount of available attached mucosa or mobile tissue [59], arch width [60], and humidity [61]. Further studies are needed to evaluate the influence of the scanning pattern on the scanning accuracy of complete-arch intraoral implant scans.

Dental literature is unclear regarding the efficacy of splinting ISB techniques when acquiring intraoral digital implant scans [62,14]. This may be explained as additional variables must be considered such as implant position or ISB design selection [20,35]. In the present study, the experimental intraoral digital scans were obtained without splinting the ISBs. The implants of the patient selected were relatively parallel, and the inter-implant distance was favorable. The results of this study revealed a mean linear discrepancy ranging from 63 to 87 μm and a mean angular discrepancy ranging from 0.43 to 0.84 degrees. These values can be considered within the clinically acceptable discrepancy [54-57].

Dental literature has shown varying scanning trueness and precision values among the different IOSs [3,20,35,44]. Therefore, it is important to understand that if a different IOS is selected, the results of the present clinical study may vary. Additional studies are needed to further evaluate the impact of the scanning patterns on the accuracy of complete-arch implant scans. Similarly, additional operator- and patient-related factors can decrease the scanning accuracy of IOSs [18-20], not only the scanning pattern used to acquire the intraoral implant scan. It is critical to understand these influencing factors for maximizing the accuracy of the IOSs [40-43].

In the present study, these ambient environmental conditions were standardized, aiming to minimize the effect of these variables on the scanning accuracy measured. Additionally, implant scan body design [63,64], the geometry bevel feature position of the implant scan body [33], and implant scan body wear [65] can influence intraoral scanning accuracy. In this study, new implant scan bodies were used and maintained in the same position during all the data acquisition procedures. Additionally, the geometry bevel feature of the implant scan body was oriented towards the lingual surface to maximize the accuracy of the digitizing procedure [33].

A previous in vitro study has analyzed the influence of the scanning pattern on the accuracy of complete-arch implant scans obtained by using an IOS (Trios 4, v.21.3; 3Shape A/S) [21]. This study did not consider the O-Lock scanning pattern. The results revealed that the circumferential scanning pattern obtained the lowest scanning time and

number of photograms [21]. Based on the results of the present study, the O-Lock scanning pattern obtained the lowest scanning time and number of photograms. However, the circumferential group obtained lower scanning time and number of photograms than the OBL and zig-zag scanning patterns. Therefore, similar results were obtained.

The present clinical study presents several limitations, including the single patient tested. Additionally, a unique ISB and implant abutment design were considered. The implants' maxillary location must also be considered, as the scanning procedure may vary in complete-arch intraoral implant scans. Only one operator and IOS system were involved in the digital data acquisition procedures, so the obtained results can not be extrapolated to other IOS systems. Finally, the obtained results should be extrapolated with caution, considering that the linear distances between platforms was considered.[46] Additionally, the overall discrepancies of the 6 linear and angular Euclidean distances were considered. The analysis of each independent linear and angular measurement was not evaluated. Further studies are needed to evaluate the influence of the scanning pattern on the scanning accuracy of complete-arch implant scans recorded by using different IOSs.

5. Conclusions

Based on the results obtained in the present clinical study, the following conclusions were drawn:

- The scanning patterns tested influenced the trueness and precision, time, and number of photograms of complete-arch implant scans acquired by using the intraoral scanner assessed.
- The O-Lock and zig-zag scanning patterns obtained the best linear trueness values. The zig-zag scanning pattern obtained significantly better angular trueness than the O-Lock scanning pattern; however, only a 0.12 degrees mean discrepancy was observed between both scanning patterns. Therefore, the zig-zag and O-Lock scanning patterns are recommended to obtain complete-arch implant scans when using the selected IOS.
- The O-Lock scanning pattern demonstrated the lowest scanning time and number of photograms among all the scanning patterns tested.

All authors discussed the evolution and commented on the manuscript at all stages.

Clinical significance

The O-Lock or Zigzag scanning patterns are recommended to maximize scanning accuracy and reduce scanning time and number of photograms in complete-arch implant digital scans.

Funding

This research did not receive any specific grant from funding agencies in the public, commercial, or not-for-profit sectors.

CRediT authorship contribution statement

Miguel Gómez-Polo: Writing – review & editing, Writing – original draft, Supervision, Methodology, Investigation, Conceptualization. **Rocío Cascos:** Investigation, Data curation. **Rocío Ortega:** Writing – review & editing, Methodology. **Abdul B. Barmak:** Formal analysis, Data curation. **John C. Kois:** Writing – review & editing. **Jorge Alonso Pérez-Barquero:** Methodology, Data curation. **Marta Revilla-León:** Writing – review & editing, Writing – original draft, Supervision, Methodology, Conceptualization.

Declaration of competing interest

The authors declare that they have no known competing financial interests or personal relationships that could have appeared to influence the work reported in this paper.

References

[1] H.T. Shillingburg, D.A. Sather, E.L. Wilson, J.R. Cain, D.L. Mitchell, L.J. Blanco, J. C. Kessler, Fundamentals of Fixed Prosthodontics, Quintessence, Chicago, 2012 fourth ed.
[2] T.R. Schoenbaum, Implant prosthodontics: Protocols and Techniques For Fixed Implant Restorations, Quintessence, Chicago, 2022 first ed.
[3] H. Lee, J.S. So, J.L. Hochstedler, C. Ercoli, The accuracy of implant impressions: a systematic review, J. Prosthet. Dent. 100 (2008) 285–291, https://doi.org/10.1016/S0022-3913(08)60208-5.
[4] B. Frieberg, T. Jemt, U. Lekholm, Early failure in 4,641 consecutively placed Brånemark dental implants: a study from stage 1 surgery to the connection of completed prostheses, Int. J. Oral Maxillofac. Impl. 6 (1991) 142–146.
[5] R. Jaffin, C. Berman, The excessive loss of Brånemark implants in type IV bone: a 5-year analysis, J. Periodontol. 62 (1991) 2–4, https://doi.org/10.1902/jop.1991.62.1.2.
[6] M.R. Baig, Accuracy of impressions of multiple implants in the edentulous arch: a systematic review, Int. J. Oral Maxillofac. Impl. 29 (2014) 869–880, https://doi.org/10.11607/jomi.3233.
[7] J.N. Ciesco, W.F.P. Malone, J.L. Sandrik, B. Mazur, Comparison of elastomeric impression materials used in fixed prosthodontics, J. Prosthet. Dent. 45 (1981) 89–94, https://doi.org/10.1016/0022-3913(81)90018-4.
[8] J.F. McCabe, R. Storer, Elastomeric impression materials. The measurement of some properties relevant to clinical practice, Br. Dent. J. 73 (1980) 73–79, https://doi.org/10.1038/sj.bdj.4804460.
[9] M.H. Reisbeck, J. Matyas, The accuracy of highly filled elastomeric impression materials, J. Prosthet. Dent. 33 (1975) 67–72.
[10] M. Revilla-León, W. Att, M. Özcan, J. Rubenstein, Comparison of conventional, photogrammetry, and intraoral scanning accuracy of complete-arch implant impression procedures evaluated with a coordinate measuring machine, J. Prosthet. Dent. 125 (2021) 470–478, https://doi.org/10.1016/j.prosdent.2020.03.005.
[11] M. Revilla-León, J. Rubenstein, M.M. Methani, W. Piedra–Cascón, M. Özcan, W. Att, Trueness and precision of complete-arch photogrammetry implant scanning assessed with a coordinate-measuring machine, J. Prosthet. Dent. 129 (2023) 160–165, https://doi.org/10.1016/j.prosdent.2021.05.019.
[12] M. Gómez-Polo, A. Sallorenzo, R. Cascos, J. Ballesteros, A.B. Barmak, M. Revilla-León, Conventional and digital complete-arch implant impression techniques: an in vitro study comparing accuracy, J. Prosthet. Dent. (2022), https://doi.org/10.1016/j.prosdent.2022.08.028 [Epub ahead of print].
[13] M. Gómez-Polo, A.B. Barmak, R. Ortega, V. Rutkunas, J.C. Kois, M. Revilla-León, Accuracy, scanning time, and patient satisfaction of stereophotogrammetry systems for acquiring 3D dental implant positions: a systematic review, J. Prosthodont. (2023), https://doi.org/10.1111/jopr.13751 [Epub ahead of print].
[14] A. Paratelli, S. Vania, C. Gómez-Polo, R. Ortega, M. Revilla-León, M. Gómez-Polo, Techniques to improve the accuracy of complete arch implant intraoral digital scans: a systematic review, J. Prosthet. Dent. 129 (2023) 844–854, https://doi.org/10.1016/j.prosdent.2021.08.018.
[15] A. Schmidt, B. Wöstmann, M.A. Schlenz, Accuracy of digital implant impressions in clinical studies: a systematic review, Clin. Oral Impl. Res. 33 (2022) 573–585, https://doi.org/10.1111/clr.13951.
[16] P. Papaspyridakos, K. Vazouras, Y.W. Chen, E. Kotina, Z. Natto, K. Kang, K. Chochlidakis, Digital vs conventional implant impressions: a systematic review and meta-analysis, J. Prosthodont. 29 (2020) 660–678, https://doi.org/10.1111/jopr.13211.
[17] C. Wulfman, A. Naveau, C. Rignon–Bret, Digital scanning for complete-arch implant-supported restorations: a systematic review, J. Prosthet. Dent. 124 (2020) 161–167, https://doi.org/10.1016/j.prosdent.2019.06.014.
[18] M. Revilla-León, D.E. Kois, J.C. Kois, A guide for maximizing the accuracy of intraoral digital scans: part 2-Patient factors, J. Esthet. Restor. Dent. 35 (2023) 241–249, https://doi.org/10.1111/jerd.12993.
[19] M. Revilla-León, D.E. Kois, J.C. Kois, A guide for maximizing the accuracy of intraoral digital scans. part 1: operator factors, J. Esthet. Restor. Dent. 35 (2023) 230–340, https://doi.org/10.1111/jerd.12985.
[20] M. Revilla-León, A. Lanis, B. Yilmaz, J.C. Kois, G.O. Gallucci, Intraoral digital implant scans: parameters to improve accuracy, J. Prosthodont. (2023), https://doi.org/10.1111/jopr.13749 [Epub ahead of print].
[21] M. Gómez-Polo, R. Cascos, R. Ortega, A.B. Barmak, J.C. Kois, M. Revilla-León, Influence of arch location and scanning pattern on the scanning accuracy, scanning time, and number of photograms of complete-arch intraoral digital implant scans, Clin. Oral Impl. Res. 34 (2023) 591–601, https://doi.org/10.1111/clr.14069.
[22] Z. Li, R. Huang, X. Wu, Z. Chen, B. Huang, Z. Chen, Effect of scan pattern on the accuracy of complete-arch digital implant impressions with two intraoral scanners, Int. J. Oral Maxillofac. Impl. 37 (2022) 731–739, https://doi.org/10.11607/jomi.9248.
[23] A. Ender, A. Mehl, Influence of scanning strategies on the accuracy of digital intraoral scanning systems, Int. J. Comput. Dent. 16 (2013) 11–21.
[24] K.C. Oh, J.M. Park, H.S. Moon, Effects of scanning strategy and scanner type on the accuracy of intraoral scans: a new approach for assessing the accuracy of scanned data, J. Prosthodont. 29 (2020) 518–523, https://doi.org/10.1111/jopr.13158. Epub 2020 Jun 26. PMID: 32133690.

[25] L. Hardan, R. Bourgi, M. Lukomska-Szymanska, J.C. Hernández-Cabanillas, J. E. Zamarripa-Calderón, G. Jorquera, et al., Effect of scanning strategies on the accuracy of digital intraoral scanners: a meta-analysis of in vitro studies, J. Adv. Prosthodont 15 (2023) 315–332, https://doi.org/10.4047/jap.2023.15.6.315.
[26] M. Gómez-Polo, W. Piedra-Cascón, M.M. Methani, N. Quesada-Olmo, M. Farjas-Abadia, M. Revilla-León, Influence of rescanning mesh holes and stitching procedures on the complete-arch scanning accuracy of an intraoral scanner: an in vitro study, J. Dent. 110 (2021) 103690, https://doi.org/10.1016/j.jdent.2021.103690.
[27] M. Gómez-Polo, M.G. Immorlano, R. Cascos–Sánchez, R. Ortega, A.B. Barmak, J. C. Kois, M. Revilla-León, Influence of the dental arch and number of cutting-off and rescanning mesh holes on the accuracy of implant scans in partially edentulous situations, J. Dent. 137 (2023) 104667, https://doi.org/10.1016/j.jdent.2023.104667.
[28] M. Revilla-León, N. Quesada–Olmo, M. Gómez-Polo, E. Sicilia, M. Farjas-M, J. C. Abadia, J.C Kois, Influence of rescanning mesh holes on the accuracy of an intraoral scanner: an in vivo study, J. Dent. 115 (2012) 103851, https://doi.org/10.1016/j.jdent.2021.103851.
[29] M. Revilla-León, E. Sicilia, R. Agustín–Panadero, M. Gómez-Polo, J.C. Kois, Clinical evaluation of the effects of cutting off, overlapping, and rescanning procedures on intraoral scanning accuracy, J. Prosthet. Dent. (2022), https://doi.org/10.1016/j.prosdent.2021.10.017 [Epub ahead of print].
[30] J. Ma, J.E. Rubenstein, Complete arch implant impression technique, J. Prosthet. Dent. 107 (2012) 405–410, https://doi.org/10.1016/S0022-3913(12)60100-0.
[31] M. Revilla-León, J.L. Sánchez-Rubio, J. Oteo-Calatayud, M. Özcan, Impression technique for a complete-arch prosthesis with multiple implants using additive manufacturing technologies, J. Prosthet. Dent. 117 (2017) 714–720, https://doi.org/10.1016/j.prosdent.2016.08.036.
[32] D. Borbola, G. Berkei, B. Simon, L. Romanszky, G. Sersli, M. DeFee, et al., In vitro comparison of five desktop scanners and an industrial scanner in the evaluation of an intraoral scanner accuracy, J. Dent. (2023), https://doi.org/10.1016/j.jdent.2022.104391.
[33] M. Gómez-Polo, F. Álvarez, R. Ortega, C. Gómez-Polo, A.B. Barmak, J.C. Kois, M. Revilla-León, Influence of the implant scan body bevel location, implant angulation and position on intraoral scanning accuracy: an in vitro study, J. Dent. 104122 (2022) 121, https://doi.org/10.1016/j.jdent.2022.104122.
[34] M. Revilla-León, A. Gohil, A.B. Barmak, M. Gómez-Polo, J.A. Pérez–Barquero, W. Att, J.C. Kois, Influence of ambient temperature changes on intraoral scanning accuracy, J. Prosthet. Dent. (2022), https://doi.org/10.1016/j.prosdent.2022.01.012 [Epub ahead of print].
[35] M. Gómez-Polo, M.B. Donmez, G. Çakmak, B. Yilmaz, M. Revilla-León, Influence of implant scan body design (height, diameter, geometry, material, and retention system) on intraoral scanning accuracy: a systematic review, J. Prosthodont. 32 (2023) 165–180, https://doi.org/10.1111/jopr.13774.
[36] M. Menini, P. Setti, F. Pera, P. Pera, P. Pesce, Accuracy of multi-unit implant impression: traditional techniques versus a digital procedure, Clin. Oral Investig. 22 (2018) 1253–1262, https://doi.org/10.1007/s00784-017-2217-9.
[37] A. Di Fiore, R. Meneghello, L. Graiff, G. Savio, P. Vigolo, C. Monaco, Full arch digital scanning systems performances for implant-supported fixed dental prostheses: a comparative study of 8 intraoral scanners, J. Prosthodont. Res. 63 (2019) 396–403, https://doi.org/10.1016/j.jpor.2019.04.002.
[38] J.H. Lim, J.M. Park, M. Kim, S.J. Heo, J.Y. Myung, Comparison of digital intraoral scanner reproducibility and image trueness considering repetitive experience, J. Prosthet. Dent. 119 (2018) 225–232, https://doi.org/10.1016/j.prosdent.2017.05.002.
[39] G. Revell, B. Simon, A. Mennito, Z.P. Evans, W. Renne, M. Ludlow, et al., Evaluation of complete-arch implant scanning with 5 different intraoral scanners in terms of trueness and operator experience, J. Prosthet. Dent. 128 (2022) 632–638, https://doi.org/10.1016/j.prosdent.2021.01.013.
[40] M. Revilla-León, P. Jiang, M. Sadeghpour, W. Piedra–Cascón, A. Zandinejad, M. Özcan, V.R. Krishnamurthy, Intraoral digital scans-Part 1: influence of ambient scanning light conditions on the accuracy (trueness and precision) of different intraoral scanners, J. Prosthet. Dent. 124 (2020) 372–378, https://doi.org/10.1016/j.prosdent.2019.06.003.
[41] M. Revilla-León, S.G. Subramanian, M. Özcan, V.R. Krishnamurthy, Clinical study of the influence of ambient light scanning conditions on the accuracy (trueness and precision) of an intraoral scanner, J. Prosthodont. 29 (2020) 107–113, https://doi.org/10.1111/jopr.13135.
[42] M. Revilla-León, S.G. Subramanian, W. Att, V.R. Krishnamurthy, Analysis of different illuminance of the room lighting condition on the accuracy (trueness and precision) of an intraoral scanner, J. Prosthodont. 30 (2021) 157–162, https://doi.org/10.1111/jopr.13276.
[43] G. Ochoa-López, R. Cascos, J.L. Antonaya-Martín, M. Revilla-León, M. Gómez-Polo, Influence of ambient light conditions on the accuracy and scanning time of seven intraoral scanners in complete-arch implant scans, J. Dent. 121 (2022) 104138, https://doi.org/10.1016/j.jdent.2022.104138.
[44] M.A. Akl, K. Daifallah, J.A. Pérez-Barquero, A.B. Barmak, A.G. Wee, M. Revilla-León, Influence of interdental spaces and the palate on the accuracy of maxillary scans acquired using different intraoral scanners, J. Prosthodont. (2023), https://doi.org/10.1111/jopr.13748 [Epub ahead of print].
[45] L. Ciocca, R. Meneghello, C. Monaco, G. Savio, L. Scheda, M.R. Gatto, P. Baldissara, In vitro assessment of the accuracy of digital impressions prepared using a single system for full-arch restorations on implants, Int. J. Comput. Assist. Radiol. Surg. 13 (2018) 1097–1108, https://doi.org/10.1007/s11548-018-1719-5.
[46] J. Vág, Z. Nagy, B. Simon, Á. Mikolicz, E. Kövér, A. Mennito, et al., A novel method for complex three-dimensional evaluation of intraoral scanner accuracy, Int. J. Comput. Dent. 22 (2019) 239–249.
[47] Z. Nagy, B. Simon, A. Mennito, Z. Evans, W. Renne, J. Vág, Comparing the trueness of seven intraoral scanners and a physical impression on dentate human maxilla by a novel method, BMC Oral Health 20 (2020) 97, https://doi.org/10.1186/s12903-020-01090-x.
[48] R.J. Kim, J.M. Park, J.S. Shim, Accuracy of 9 intraoral scanners for complete-arch image acquisition: a qualitative and quantitative evaluation, J. Prosthet. Dent. 120 (2018) 895–903, https://doi.org/10.1016/j.prosdent.2018.01.035.
[49] F.G. Mangano, U. Hauschild, G. Veronesi, M. Imburgia, C. Mangano, O. Admakin, Trueness and precision of 5 intraoral scanners in the impressions of single and multiple implants: a comparative in vitro study, BMC Oral Health 19 (2019) 101, https://doi.org/10.1186/s12903-019-0792-7.
[50] P. Medina-Sotomayor, A. Pascual-Moscardó, I. Camps, Accuracy of four digital scanners according to scanning strategy in complete-arch impressions, PLoS ONE 13 (2018) e0202916, https://doi.org/10.1371/journal.pone.0202916.
[51] M. Revilla-León, A. Gohil, A.B. Barmak, A. Zandinejad, A.J. Raigrodski, J. Alonso Pérez–Barquero, Best-fit algorithm influences on virtual casts' alignment discrepancies, J. Prosthodont. (2022), https://doi.org/10.1111/jopr.13537 [Epub ahead of print].
[52] Accuracy (trueness and precision) of Measurement Methods and Results - Part 1: General principles and Definitions, International Organization for Standardization, 1994. https://www.iso.org/obp/ui/#iso:std:iso:5725:-1:ed-1:v1:en. Accessed 02-01-20.
[53] Dentistry - Digital impression Devices - Part 1: Methods for Assessing Accuracy, International Organization for Standardization, 2019. https://www.iso.org/standard/69402.html. Accessed 02-01-20.
[54] J. Katsoulis, T. Takeichi, A.S. Gaviria, L. Peter, K. Katsoulis, Misfit of implant protheses and its impact on clinical outcomes. Definition, assessment and a systematic review of the literature, Eur. J. Oral Implantol. 10 (2017) 121–138.
[55] T. Jemt, A. Lie, Accuracy of implant-supported prostheses in the edentulous jaw: analysis of precision of fit between cast gold-alloy frameworks and master casts by means of a three-dimensional photogrammetric technique, Clin. Oral Impl. Res. 6 (1995) 172–180, https://doi.org/10.1034/j.1600-0501.1995.060306.x.
[56] S. Vandeweghe, V. Vervack, M. Dierens, H. De Bruyn, Accuracy of digital impressions of multiple dental implants: an in vitro study, Clin. Oral Impl. Res. 28 (2017) 648–653, https://doi.org/10.1111/clr.12853.
[57] A.L. Carneiro Pereira, V.R. Medeiros, A. da Fonte Porto Carreiro, Influence of implant position on the accuracy of intraoral scanning in fully edentulous arches: a systematic review, J. Prosthet. Dent. 126 (2021) 749–755, https://doi.org/10.1016/j.prosdent.2020.09.008.
[58] M. Gómez-Polo, A. Sallorenzo, R. Ortega, C. Gómez-Polo, A.B. Barmak, W. Att, M. Revilla-León, Influence of implant angulation and clinical implant scan body height on the accuracy of complete arch intraoral digital scans, J. Prosthet. Dent. (2022), https://doi.org/10.1016/j.prosdent.2021.11.018 [Epub ahead of print].
[59] V. Rasaie, J. Abduo, S. Hashemi, Accuracy of intraoral scanners for recording the denture bearing areas: a systematic review, J. Prosthodont. 30 (2021) 520–539, https://doi.org/10.1016/j.prosdent.2021.11.018.
[60] N. Kaewbuasa, C. Ongthiemsak, Effect of different arch widths on the accuracy of three intraoral scanners, J. Adv. Prosthodont. 13 (2021) 205–215, https://doi.org/10.4047/jap.2021.13.4.205.
[61] M. Gómez-Polo, R. Ortega, A. Sallorenzo, R. Agustín-Panadero, A.B. Barmak, J. C. Kois, M. Revilla-León, Influence of the surface humidity, implant angulation, and interimplant distance on the accuracy and scanning time of complete-arch implant scans, J. Dent. 127 (2022) 104307, https://doi.org/10.1016/j.jdent.2022.
[62] R. Nedelcu, P. Olsson, M. Thulin, I. Nyström, A. Thor, In vivo trueness and precision of full-arch implant scans using intraoral scanners with three different acquisition protocols, J. Dent. 128 (2023) 104308, https://doi.org/10.1016/j.jdent.2022.104308.
[63] R.M. Mizumoto, B. Yilmaz, Intraoral scan bodies in implant dentistry: a systematic review, J. Prosthet. Dent. 120 (2018) 343–352, https://doi.org/10.1016/j.prosdent.2017.10.029.
[64] M. Moslemion, L. Payaminia, H. Jalali, M. Alikhasi, Do type and shape of scan bodies affect accuracy and time of digital implant impressions? Eur J Prosthodont. Restor. Dent. 28 (2020) 18–27, https://doi.org/10.1922/EJPRD_1962Moslemion10. PMID: 32036633.
[65] L. Arcuri, F. Lio, V. Campana, V. Mazzetti, F.R. Federici, A. Nardi, M. Galli, Influence of implant scanbody wear on the accuracy of digital impression for complete-arch: a randomized in vitro trial, Materials (Basel) 15 (2022) 927, https://doi.org/10.3390/ma15030927.